

DOI 10.24425/ae.2020.133032

Battery/super-capacitor HESS applied in DC microgrid

ZHEN ZHANG , BAUGE ZHANG, DONGHAO WANG, PING LI, YAO RONG

Lanzhou Jiaotong University
China

e-mail: zhangz0914@163.com

(Received: 4.11.2019, revised: 18.12.2019)

Abstract: Energy storage technology (EST) is an effective way to improve the power quality of renewable energy generation (such as solar energy and wind energy), but a single energy storage system (ESS) is difficult to meet the demand for the safe operation of the grid. According to the structure and operation characteristics of the existing battery/super-capacitor hybrid energy storage system (HESS), a battery/super-capacitor HESS is proposed. The working principle and three working modes (the super-capacitor pre-charging cold stand-by mode, the boost mode and buck mode) of the HESS are analyzed in detail. The state equations of the boost mode and buck mode are derived. The state space average method is used to establish the small signal equivalent model under the buck/boost mode. Moreover, the charge and discharge control strategy of the HESS is obtained by combining the voltage closed-loop control. The simulation model is built in Matlab/Simulink to verify the effectiveness of the proposed HESS and its control strategy. The results show that the HESS and its control strategy can ensure the DC bus voltage has good stability and superior anti-interference, and it can simultaneously provide large current, increase the battery life, and improve the technical economy of energy storage.

Key words: battery, bi-directional DC/DC converter, HESS, super-capacitor, voltage closed-loop

1. Introduction

With the large amount of renewable energy utilized in the grid, renewable energy power generation (such as solar energy and wind energy) is going to play an indispensable role in the future development of the power system [1]. However, the output power of distributed generation (DG) units are intermittent and random, which brings new challenges to the safe and stable



© 2020. The Author(s). This is an open-access article distributed under the terms of the Creative Commons Attribution-NonCommercial-NoDerivatives License (CC BY-NC-ND 4.0, <https://creativecommons.org/licenses/by-nc-nd/4.0/>), which permits use, distribution, and reproduction in any medium, provided that the Article is properly cited, the use is non-commercial, and no modifications or adaptations are made.

operation of the power system [2, 3]. Energy storage technology (EST) with the function of “peak cutting and valley filling” is an effective way to solve the power quality of renewable energy generation, and it is also the key technology to ensure the safe and stable operation of the grid [4].

The hybrid energy storage system (HESS) has been becoming a hot research topic because it can overcome the limitations of the single energy storage system (ESS) (low power density, low energy density, slow effect speed and short life, etc.) and combine the advantages of both [5]. The ESS is mainly composed of two parts: an energy storage unit and a bi-directional DC/DC converter [6]. A battery ESS can reduce the fluctuation of wind energy output in wind power generation, but the power density of the battery is low [7]. A super-capacitor ESS can realize the storage of regenerative braking energy in urban rail transit, but the low energy density of the super-capacitor may affect the safe and stable operation of the train [8]. An isolated bi-directional DC/DC converter can achieve high power density and current isolation, but when the isolation transformer exists, the leakage inductance and control of the transformer should be considered [9]. Authors of [10] have proposed a high ratio DC/DC converter, which can effectively reduce the voltage stress of the switch. A high-power bi-directional DC/DC converter for distributed photovoltaic power generation has been suggested by [11], which can maximize the solar energy collection capacity. An HESS of a battery and super-capacitor has been presented [12], which effectively combines the advantages of both and reduces the impact of wind energy fluctuation. However, the HESS is a parallel two independent branches with complex control and poor economy. The application of the HESS in the grid is investigated [13–15]. The results show that the HESS can effectively combine the advantages of a battery and super-capacitor, stabilize the stable operation of the grid and improve the battery life.

Based on the study of energy storage requirements for safe and stable operation of a DC microgrid, this paper proposes a battery/super-capacitor HESS, which adopts voltage closed-loop control to improve the voltage stability of a DC bus and the anti-interference performance of the HESS. This paper compares the recovery effect of the HESS and battery ESS on the DC bus voltage to illustrate the advantages of the HESS. The specific arrangement of the paper is as follows: Section 2 exhibits the topological structure and working principle of the proposed HESS, while section 3 displays the control strategy of the HESS. Section 4 introduces the simulation results and analysis of the system. Finally, section 5 summarizes the article and shows the next work.

2. System configuration and working principle

2.1. System configuration

The HESS shares a set of a DC/DC converter, adds a diode D with the function of selective switch, and adds a separate pre-charging circuit as cold stand-by to ensure the normal operation of the super-capacitor. The specific topology is shown in Fig. 1. Among them, U_E and U_C are the battery and super-capacitor terminal voltages, respectively, and U_d is the DC bus terminal voltage.

2.2. Working modes of the system

The HESS has three working modes: the super-capacitor pre-charging cold stand-by mode, the boost mode and buck mode.

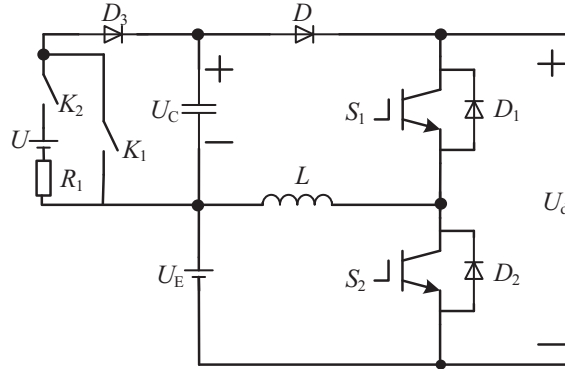


Fig. 1. Structure of battery-super-capacitor HESS

Case 1: the super-capacitor pre-charging cold stand-by mode

When the system is in the stand-by state, provided that U_C is detected to be in safe working voltage, K_1 is closed and K_2 is opened. The equivalent circuit diagram is shown in Fig. 2(a). As can be seen from Fig. 2(a), D_3 is cut off due to reverse voltage U_C , and the super-capacitor pre-charge circuit will not work [16]. Provided that U_C is detected to be lower than the cut-off voltage, K_1 is opened and K_2 is closed. The equivalent circuit diagram is shown in Fig. 2(b). As can be seen from Fig. 2(b), D is cut off due to reverse voltage, and the super-capacitor is in the pre-charge mode.

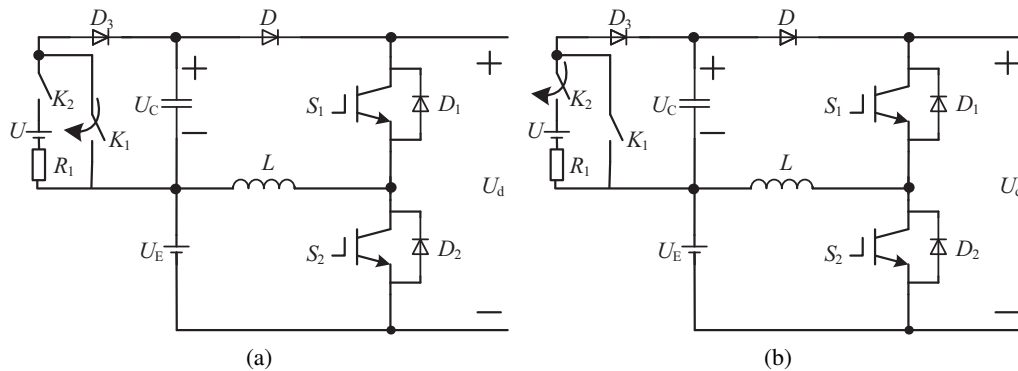


Fig. 2. Equivalent circuit diagram in supercapacitor pre-charging mode: working state 1 (a); working state 2 (b)

The super-capacitor pre-charging mode is actually a first-order RC circuit. Power supply U (power supply U is actually introduced from the DC bus voltage to improve the economy of ESS) charges the super-capacitor through discharge resistance R_1 . Meanwhile, the pre-charge circuit of the proposed topology has been applying the pre-charge of capacitor voltage in the sub-module of the modular multilevel converter.

Case 2: the buck mode

When the DC bus voltage rises, the system operates in the buck mode. Its equivalent circuit diagram is shown in Fig. 3. In buck mode, the anti-parallel diode D_2 of switch S_2 and switch S_1 works alternately.

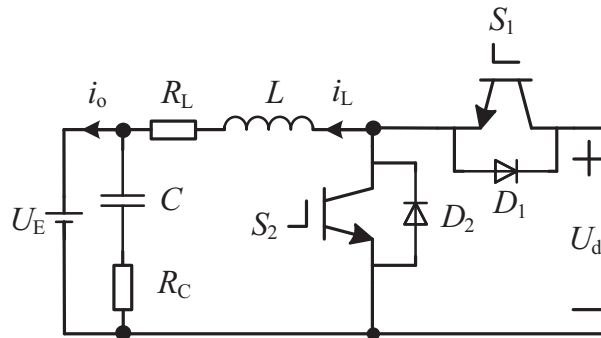


Fig. 3. Equivalent circuit diagram of buck mode

Define switch function S :

$$S = \begin{cases} 1 & \text{the } S_1 \text{ or } S_2 \text{ is turned on} \\ 0 & \text{the } S_1 \text{ or } S_2 \text{ is turned off} \end{cases} \quad (1)$$

According to Fig. 3, the corresponding equation of the state can be obtained as follows:

$$\begin{pmatrix} \frac{di_L}{dt} \\ \frac{du_C}{dt} \end{pmatrix} = \begin{pmatrix} \frac{1}{L} & -\frac{R_L}{L} \\ 0 & \frac{1}{C} \end{pmatrix} \begin{pmatrix} S U_d \\ i_L \end{pmatrix} + \begin{pmatrix} -\frac{1}{L} & 0 \\ 0 & -\frac{1}{C} \end{pmatrix} \begin{pmatrix} U_E \\ i_o \end{pmatrix} \quad (2)$$

According to Equation (2) and the state space average method [17], the corresponding average equation can be obtained:

$$\begin{pmatrix} \frac{di_L}{dt} \\ \frac{du_C}{dt} \end{pmatrix} = \begin{pmatrix} D & -\frac{R_L}{L} \\ 0 & \frac{1}{C} \end{pmatrix} \begin{pmatrix} U_d \\ i_L \end{pmatrix} + \begin{pmatrix} -\frac{1}{L} & 0 \\ 0 & -\frac{1}{C} \end{pmatrix} \begin{pmatrix} U_E \\ i_o \end{pmatrix}, \quad (3)$$

where: $D = t_{on}/(t_{on} + t_{off})$, is the duty cycle of S_1 .

Added disturbance:

$$\begin{cases} d = D + \hat{d} \\ i_L = I_L + \hat{i}_L \\ u_d = U_d + \hat{u}_d \\ u_E = U_E + \hat{u}_E \\ u_C = U_C + \hat{u}_C \end{cases} \quad (4)$$

By substituting Formula (3), the small signal transfer function of control-voltage can be obtained through the Laplace transformation:

$$G_{vd1} = \frac{\hat{u}_E(s)}{\hat{d}(s)} \Big|_{\hat{u}_d(s)=0} = \frac{U_d(s)}{LCs^2 + R_LCs + 1}. \quad (5)$$

Case 3: the boost mode

When the DC bus voltage decreases, the system operates in the boost mode. Its equivalent circuit diagram is shown in Fig. 4. In the boost mode, the anti-parallel diode D_1 of switch S_1 and switch S_2 works alternately.

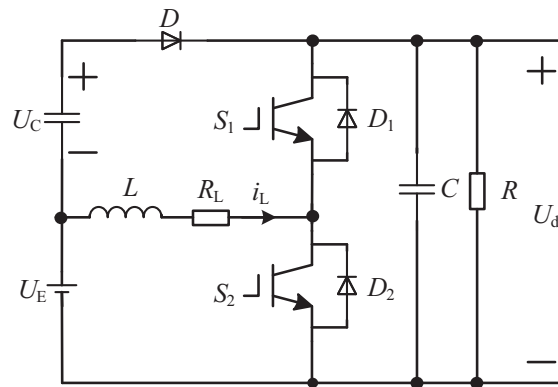


Fig. 4. Equivalent circuit diagram of boost mode

According to Fig. 4, the corresponding equation of the state can be obtained as follows:

$$\begin{pmatrix} \frac{di_L}{dt} \\ \frac{du_d}{dt} \end{pmatrix} = \begin{pmatrix} -\frac{(1-S)}{L} & -\frac{R_L}{L} \\ -\frac{1}{RC} & \frac{(1-S)}{C} \end{pmatrix} \begin{pmatrix} U_d \\ i_L \end{pmatrix} + \begin{pmatrix} \frac{1}{L} \\ 0 \end{pmatrix} U_E. \quad (6)$$

According to Equation (6) and the state space average method, the corresponding average equation can be obtained:

$$\begin{pmatrix} \frac{di_L}{dt} \\ \frac{du_d}{dt} \end{pmatrix} = \begin{pmatrix} -\frac{(1-D)}{L} & -\frac{R_L}{L} \\ -\frac{1}{RC} & \frac{(1-D)}{C} \end{pmatrix} \begin{pmatrix} U_d \\ i_L \end{pmatrix} + \begin{pmatrix} \frac{1}{L} \\ 0 \end{pmatrix} U_E, \quad (7)$$

where: $D = t_{on}/(t_{on} + t_{off})$, is the duty cycle of S_2 .

By substituting Formula (4) into Formula (7), the small signal transfer function of control-voltage can be obtained through the Laplace transformation.

$$G_{vd2} = \frac{\hat{u}_d(s)}{\hat{d}(s)} \Big|_{\hat{u}_d(s)=0} = \frac{U_d(s) \left(D' - \frac{R_L + sL}{RD'} \right)}{LCs^2 + \left(R_LC + \frac{L}{R} \right) s + \frac{R_L}{R} + D'}, \quad (8)$$

where: $D' = 1 - D$.

3. Control strategy

The energy management of the HESS mainly depends on the control strategy of a bi-directional DC/DC converter, that is, the charge and discharge of a battery and super-capacitor bank are realized by controlling the bi-directional DC/DC converter. It is the core of control to keep the voltage of the DC bus constant. In this paper, the voltage closed-loop control is used to make the DC bus voltage stable at the rated voltage quickly. The way to generate the control pulse of the bi-directional DC/DC converter is mainly composed of complementary pulse width modulation (PWM) and independent PWM. The difference between them is whether the driving signals of S_1 and S_2 are complementary. In order to improve the stability of the system, the independent PWM mode is used.

The bi-directional DC/DC converter control strategy of the HESS consists of two parts: a logic judgment unit and a voltage closed-loop control unit. The specific control block diagram is shown in Fig. 5. When the voltage U_d suddenly rises (such as locomotive braking process), the difference ΔU_{d1} between the reference voltage U_d^* at the DC bus and the actual value U_d , then the theoretical duty cycle d_1' is obtained through PI and the limiting link, and then the current actual duty ratio d_1 is obtained by combining the independent PWM mode. At this time, the HESS works in the buck mode, S_2 is off, S_1 is in PWM. When the voltage U_d suddenly drops (such as the starting process of the locomotive), the difference ΔU_{d2} between the reference voltage U_d^* at the DC bus and the actual value U_d , then the theoretical duty cycle d_2' is obtained through the proportional-integral (PI) and limiting link, and then the current actual duty ratio d_2 is obtained by combining the independent PWM mode. At this time, the HESS works in the boost mode, S_1 is off, S_2 is in the PWM. The PI is used to realize the tracking control of U_d at the DC bus to U_{dref} .

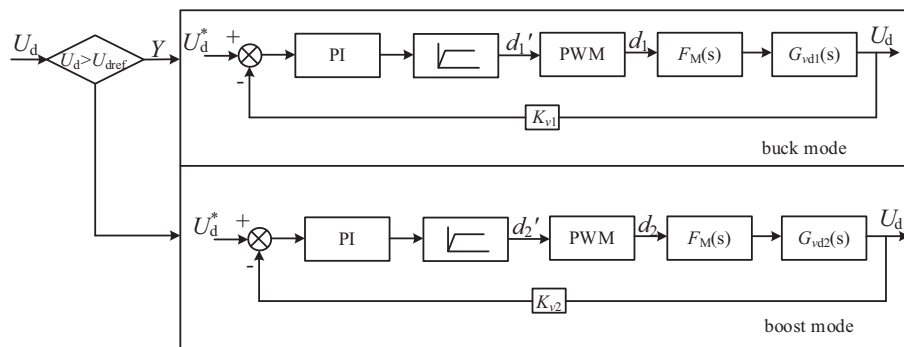


Fig. 5. Control strategy block diagram of bi-directional DC/DC converter for HESS

3.1. Simulation results and discussion

In order to verify the effectiveness of the HESS and its control strategy, Matlab/Simulink scientific computing environment was used to simulate, and the main simulation parameters of the system are shown in Table 1.

Fig. 6 shows the pre-charge waveform of the super-capacitor when the discharge depth of the super-capacitor is 50%. From Fig. 6, it can be seen that when the super-capacitor voltage is

Table 1. Main simulation parameters of the system

Parameter name	Symbol	Value	Unit
Battery voltage	U_E	48	V
Super-capacitor voltage	U_C	48	V
DC bus voltage	U_d	120	V
Inductance	L	8.2×10^{-5}	H
Discharge resistance	R_1	6.94×10^{-5}	Ω
Output capacitance	C	3.76	mF

detected to be reduced to 24 V or below, the super-capacitor pre-charging circuit is activated to charge the super-capacitor. At 600 ms, the super-capacitor voltage reaches 47.2 V, and the power supply will be restored to the normal working voltage. Meanwhile, the pre-charge time of the super-capacitor is within a reasonable range [18].

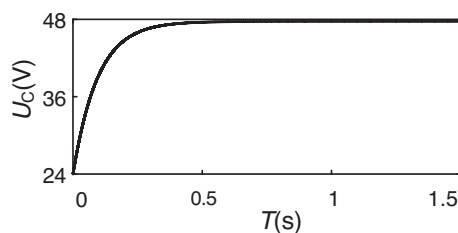


Fig. 6. Pre-charging waveform of super-capacitor

Case 1: no load disturbance

When the DC bus voltage suddenly decreases (such as the moment of motor start, etc.), the system works in the boost mode. Fig. 7 shows the waveform of the DC bus voltage U_d of the HESS and the battery ESS in the boost mode when the DC bus voltage is reduced to 90 V. It can be seen from Fig. 7 that under the HESS, the maximum voltage U_d at the DC bus is 134.1 V, and the U_d stability value is 120 V; the system overshoot is about 11.6%; the system regulation time is 0.95 ms; the voltage ripple is about 0.73%, less than 2%. Under the battery ESS, the stable value of the DC bus voltage U_d is 123.9 V, the stable value of U_d is 119.8 V; the system overshoot is about 3.5%; the system regulation time is 1.45 ms. The regulation time of the battery ESS is 34.5% longer than that of the HESS. Therefore, the DC bus voltage recovery effect and dynamic performance of the HESS in the boost mode are better than that of the battery ESS.

When the DC bus voltage suddenly increases (such as locomotive braking process, etc.), the system works in the buck mode. Fig. 8 shows the waveform of the DC bus voltage U_d in the buck mode when the DC bus voltage increases by 150 V. It can be seen from Fig. 8 that under this condition, the stable value of the DC bus voltage U_d is 118.55 V; the system overshoot is about 11.25%; the system regulation time is 0.8 ms; the voltage ripple is about 0.75%, less than 2%.

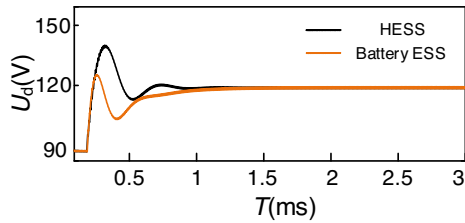


Fig. 7. Waveform of boost mode

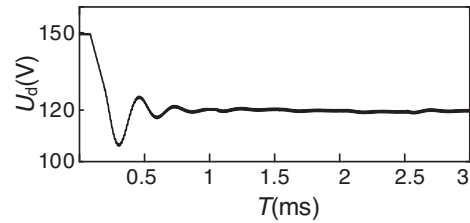


Fig. 8. Waveform of buck mode

Case 2: adding load disturbance

When the DC bus voltage suddenly decreases (such as the moment of motor start, etc.), the system works in the boost mode. A periodic load disturbance is added at 1 ms to decrease the DC bus voltage, and a periodic load disturbance is added at 2 ms to increase the DC bus voltage. Fig. 9 shows the waveform of the voltage U_d at the DC bus of the proposed HESS in the boost mode when the load disturbance is added. It can be seen from Fig. 9 that the voltage at the DC bus drops to 111.8 V in 1 ms and recovers to 120 V after 0.305 ms; the voltage at the DC bus rises to 129.5 V in 2 ms and recovers to 120 V after 0.385 ms.

When the DC bus voltage suddenly increases (such as locomotive braking process, etc.), the system works in buck mode. A periodic load disturbance is added at 1 ms to decrease the DC bus voltage, and a periodic load disturbance is added at 2 ms to increase the DC bus voltage. Fig. 10 shows the waveform of the DC bus voltage U_d in buck mode of the proposed HESS when the load disturbance is added. It can be seen from Fig. 10 that the voltage at the DC bus drops to 114.3 V in 1 ms and recovers to 119.8 V after 0.41 ms; the voltage at the DC bus side rises to 126.3 V in 2 ms and recovers to 119.8 V after 0.39 ms.

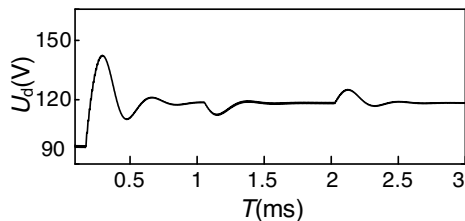


Fig. 9. Waveform of boost mode with load disturbance

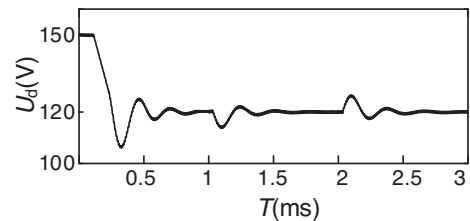


Fig. 10. Waveform of buck mode with load disturbance

4. Conclusion

Maintaining a constant DC bus voltage is the first prerequisite for the safe and stable operation of the DC microgrid. In this paper, the HESS and its control strategy are analyzed in theory and simulation. The results demonstrate that the HESS and its control strategy can increase the service life of the battery, reduce the size of the battery, and improve the economy of the ESS. Simultaneously, the super-capacitor pre-charge cold standby state and the boost, buck mode work

independently. The diode D with the function of a selective switch can charge the main power battery, and the super-capacitor pre-charge circuit, as the cold standby, effectively guarantees the performance of the super-capacitor. In addition, the voltage ripple of the HESS and its control strategy is small, while the voltage stabilizing effect and the anti-interference performance is superior.

Finally, the next step is to verify the proposed HESS in practical engineering, and further discuss and analyze the coordinated control strategy of the HESS for a microgrid.

Acknowledgements

This research work is supported by National Natural Science Foundation of China (No. 61741508). We would like to thank the China Scholarship Council for the financial support and Foundation of A Hundred Youth Talents Training Program of Lanzhou Jiaotong University.

References

- [1] Telukunta V., Pradhan J., Agrawal A., Singh M., Srivani S.G., *Protection challenges under bulk penetration of renewable energy resources in power systems: A review*, CSEE Journal of Power and Energy Systems, vol. 3, no. 4, pp. 365–379 (2017), DOI: 10.17775/CSEEJPES.2017.00030.
- [2] Zhang C., Chen H., Liang Z., Mo W., Zheng X., Hua D., *Interval voltage control method for transmission systems considering interval uncertainties of renewable power generation and load demand*, IET Generation, Transmission and Distribution, vol. 12, no. 17, pp. 4016–4025 (2018), DOI: 10.1049/iet-gtd.2018.5419.
- [3] Fan M., Sun K., Lane D., Gu W., Li Z., Zhang F., *A Novel Generation Rescheduling Algorithm to Improve Power System Reliability with High Renewable Energy Penetration*, IEEE Transactions on Power Systems, vol. 33, no. 3, pp. 3349–3357 (2018), DOI: 10.1109/TPWRS.2018.2810642.
- [4] Zhang Z., Zhang Y., Huang Q., Lee W., *Market-oriented optimal dispatching strategy for a wind farm with a multiple stage hybrid energy storage system*, CSEE Journal of Power and Energy Systems, vol. 4, no. 4, pp. 417–424 (2018), DOI: 10.17775/CSEEJPES.2018.00130.
- [5] Yan N., Zhang B., Li W., Ma S., *Hybrid Energy Storage Capacity Allocation Method for Active Distribution Network Considering Demand Side Response*, IEEE Transactions on Applied Superconductivity, vol. 29, no. 2, pp. 1–4 (2019), DOI: 10.1109/TASC.2018.2889860.
- [6] Jiang W., Zhu C., Yang C., Zhang L., Xue S., Chen W., *The Active Power Control of Cascaded Multilevel Converter Based Hybrid Energy Storage System*, IEEE Transactions on Power Electronics, vol. 34, no. 8, pp. 8241–8253 (2019), DOI: 10.1109/TPEL.2018.2882450.
- [7] Zhang Y., Iu H.H., Fernando T., Yao F., Emami K., *Cooperative Dispatch of BESS and Wind Power Generation Considering Carbon Emission Limitation in Australia*, IEEE Transactions on Industrial Informatics, vol. 11, no. 6, pp. 1313–1323 (2015), DOI: 10.1109/TII.2015.2479577.
- [8] Yang Z., Yang Z., Xia H., Lin F., *Brake Voltage Following Control of Supercapacitor-Based Energy Storage Systems in Metro Considering Train Operation State*, IEEE Transactions on Industrial Electronics, vol. 65, no. 8, pp. 6751–6761 (2018), DOI: 10.1109/TIE.2018.2793184.
- [9] He P., Khaligh A., *Comprehensive analyses and comparison of 1 kW isolated DC-DC converters for bidirectional EV charging systems*, IEEE Transactions on Transportation Electrification, vol. 3, no. 1, pp. 147–156 (2017).
- [10] Kim K., Cha H., Park S., Lee I., *A Modified Series-Capacitor High Conversion Ratio DC-DC Converter Eliminating Start-Up Voltage Stress Problem*, IEEE Transactions on Power Electronics, vol. 33, no. 1, pp. 8–12 (2018), DOI: 10.1109/TPEL.2017.2705705.

- [11] Suntio T., Kuperman A., *Comments on An Efficient Partial Power Processing DC/DC Converter for Distributed PV Architectures*, IEEE Transactions on Power Electronics, vol. 30, no. 4, pp. 2372–2372 (2015), DOI: 10.1109/TPEL.2014.2327018.
- [12] Wang J., Xu Y., Lv M., *Modeling and simulation analysis of hybrid energy storage system based on wind power generation system*, IEEE:2018 International Conference on Control, Automation and Information Sciences (ICCAIS), Hangzhou, China, pp. 422–427 (2018).
- [13] Bahloul M., Khadem S.K., *Impact of Power Sharing Method on Battery Life Extension in HESS for Grid Ancillary Services*, IEEE Transactions on Energy Conversion, vol. 34, no. 3, pp. 1317–1327 (2019), DOI: 10.1109/TEC.2018.2886609.
- [14] Xiao J., Wang P., Setyawan L., *Multilevel Energy Management System for Hybridization of Energy Storages in DC Microgrids*, IEEE Transactions on Smart Grid, vol. 7, no. 2, pp. 847–856 (2016), DOI: 10.1109/TSG.2015.2424983.
- [15] Ma W., *Optimal Allocation of Hybrid Energy Storage Systems for Smoothing Photovoltaic Power Fluctuations Considering the Active Power Curtailment of Photovoltaic*, IEEE Access, vol. 7, pp. 74787–74799 (2019), DOI: 10.1109/ACCESS.2019.2921316.
- [16] Li B.B., Xu D.D., Zhang Y., Yang R.F., Wang G.L., Xu D.G., *Closed-loop pre-charge control of modular multilevel converters during start-up processes*, IEEE Transactions on Power Electronics, vol. 30, no. 2, pp. 524–531 (2015), DOI: 10.1109/TPEL.2014.2334055.
- [17] Wang L., *Electromagnetic Transient Modeling and Simulation of Power Converters Based on a Piecewise Generalized State Space Averaging Method*, IEEE Access, vol. 7, pp. 12241–12251 (2019), DOI: 10.1109/ACCESS.2019.2891122.
- [18] Chen P.P., Wang X.Q., *Design of Pre-charge Resistor Selection for Power Battery*, Bus and Coach Technology and Research, vol. 40, no. 01, pp. 30–33 (2018), DOI: 10.15917/j.cnki.1006-3331.2018.01.009.